Identifying historical climate changes through spatial analogs

Andrew D. King[1]

1. ARC Centre of Excellence for Climate Extremes and School of Geography, Earth and Atmospheric Sciences, University of Melbourne, Melbourne, Australia.

Corresponding Author: Andrew King (andrew.king@unimelb.edu.au)

Key Points

- Climate analogs have been used as a projection tool. Here, analogs are computed using Australian observations to identify past changes.
- There is already evidence for significant changes in climate in Australian cities using analogs, particularly where rainfall has changed.
- Climate analogs provide a singular measure of multivariate changes which may be tailored to meet individual stakeholder requirements.

Abstract

Spatial analogs have previously been used to communicate climate projections by comparing the future climate of a location with an analogous recent climate at a different location which is typically hotter. In this study, spatial climate analogs were computed using observational data to identify and quantify past changes. A sigma dissimilarity metric was computed to compare the recent climates of nine major Australian cities and early 20th century climate. Evidence of climate shifts is found, particularly in locations, such as Perth, where precipitation has significantly changed in addition to the warming trend observed at all cities. Analogs designed to capture extremes, including a human health-relevant climate analog, were constructed and these also highlight significant climate shifts. This work demonstrates the utility of climate analogs for monitoring past climate changes as well as examining future change. Tailored analogs could be studied to communicate climate changes relevant to specific stakeholders.

Plain Language Summary

Future climates of cities are frequently compared with the current climates of other cities. In this work, I see if I can compare the current climates of Australian cities with other locations' climates in the past. I found that this method can be used to identify and quantify past climate change in observational data. The climate analogs can be made to represent different characteristics of the climate, so could be designed to be useful for specific industries.

1. Introduction

The world is warming due to anthropogenic greenhouse gas emissions. To date, the planet has warmed by around 1.1°C relative to pre-industrial levels (IPCC, 2021). Global warming has been accompanied by local warming across almost all of the world and significant precipitation changes in some locations as well as other earth system changes. Scientists have used observational datasets to quantify changes in the climate to date and compute other relevant metrics beyond trends, such as climate emergence statistics (Hawkins et al., 2020; Mahlstein et al., 2012).

As greenhouse gas emissions remain close to record high levels (Davis et al., 2022; Friedlingstein et al., 2022) and global warming will continue as long as greenhouse gas emissions remain significantly net-positive (King et al., 2022; MacDougall et al., 2020), further warming and other climate changes are expected over the coming decades. Climate projections are made based on model simulations to provide estimates of future local changes. Projections are communicated in different ways, but one popular method is spatial climate analogs. Analogs have been used to illustrate changes by projecting that a location's climate may become more like another location's, typically hotter, current climate, if greenhouse gas emissions continue. The use of analogs has been popular for examining different climate impacts including in climate-sensitive industries such as health (Kalkstein & Greene, 1997) and agriculture (Bergthórsson et al., 1988; Webb et al., 2013). Climate analogs have previously been computed from global and regional downscaled model simulations and are used by organizations including Copernicus (https://climate-analogues.climate.copernicus.eu/) and the Commonwealth Scientific and Industrial Research Organisation (CSIRO) in Australia (https://www.climatechangeinaustralia.gov.au/en/projections-tools/climate-analogues/) to display analogous climates for locations under different greenhouse gas emissions scenarios for the 21st century. Spatial climate analogs are relatively straightforward to communicate and understand and may be computed based on multiple variables.

In this study, I investigated whether climate analogs may be used to identify *past* climate changes in observational datasets, rather than their common use for projections. In this instance, the recent climate of a location was compared with the climate at all locations in the past to identify the best historical analog. Analysis of historical climate analogs supports previous work to understand the extent of climate changes to date, such as emergence metrics, and provides a framework for their use for climate monitoring efforts. Here, I computed climate analogs for nine major cities in Australia (Figure 1a).

Australia is a continent with diverse local climates, including tropical, arid and temperate climate types (Peel et al., 2007), and population centres spread across these climates. Annual-average temperatures vary from below 10°C in mountainous parts of the southeast of the continent to above 28°C in the tropical north (Figure 1a). Precipitation varies with the arid interior receiving less than 1mm/day whereas some coastal and high-altitude areas experience more than 6mm/day on average (Figure 1b). Australia has also warmed (Figure 1c-f), especially the southern half of the continent in spring and summer, with temperatures rising an average of about 1.4°C since 1910 (Australian Bureau of

Meteorology, 2020b). Precipitation change has been more spatially variable with increases in the north and interior and drying in the coastal south (Figure 1g-j). Australia's diverse climate and significant climate changes in the observed record make it a suitable study region for examining for past spatial climate analogs to the recent climate.

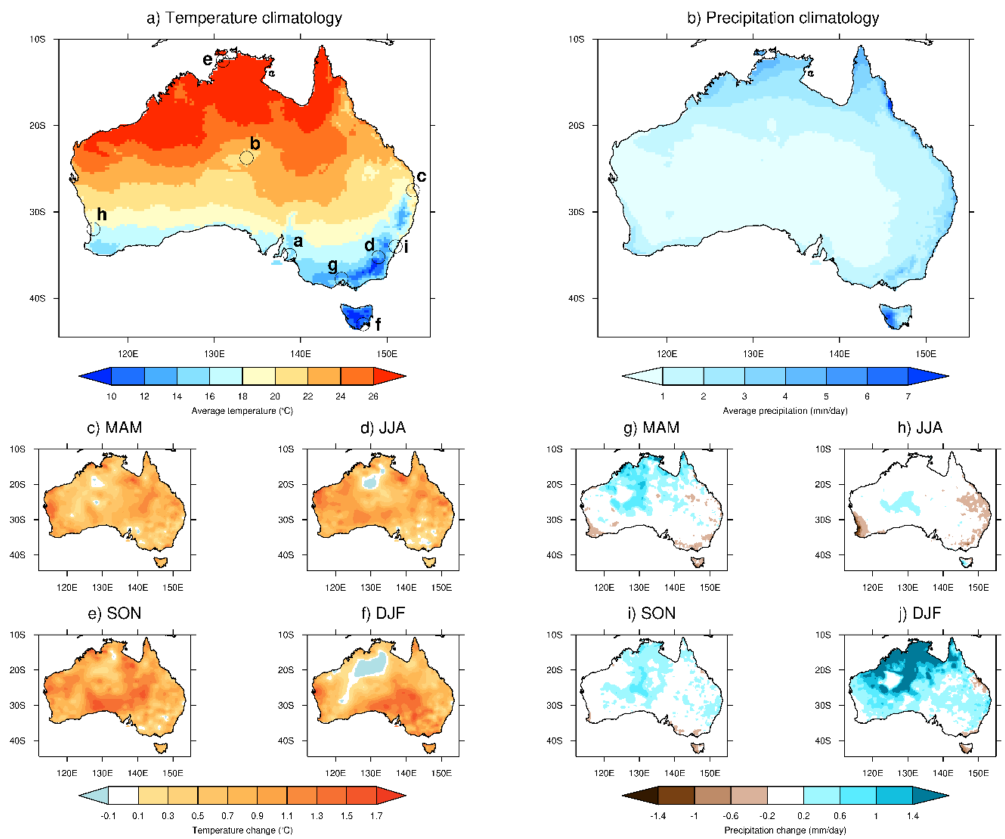

Figure 1. Maps of (a) average temperatures and (b) average precipitation across Australia for 1991-2020. Cities for which analogs are computed are marked in (a) in alphabetical order: 'a' for Adelaide, 'b' for Alice Springs, 'c' for Brisbane, 'd' for Canberra, 'e' for Darwin, 'f' for Hobart, 'g' for Melbourne, 'h' for Perth, and 'i' for Sydney. (c-f) Changes in seasonal-average temperatures between 1910-1937/38 and 1994-2021/22 for March-May, June-August, September-November, and December-February respectively. (g-j) Changes in seasonal-average precipitation rates between 1910-1937/38 and 1994-2021/22 for March-May, June-August, September-November, and December-February respectively.

2. Data and Methods

2.1. Observational data

Observational data from the Australian Gridded Climate Dataset (AGCD; Evans et al., 2020; Jones et al., 2009) were used in this study. Gridded observational data for daily precipitation totals, maximum temperature and minimum temperature from January 1910-August 2022 were interpolated from a native regular grid of 0.01° to 0.25° using a conservative regridding method. The data were separated into the four meteorological seasons: March-May (MAM), June-August (JJA), September-November (SON) and December-February (DJF). Five sets of climate analogs were computed for which results are shown here:

1. Seasonal mean temperatures and total precipitation values were calculated and these eight variables formed the basis of the mean climate analogs analysis.
2. To better understand the mean climate analog results, analogs computed from only the four seasonal mean temperature variables were also computed.
3. Similarly, analogs were computed for only the four precipitation variables too.
4. The first climate extremes analog used eight variables based on two indices recommended by the Expert Team on Climate Change Detection and Indices (ETCCDI): seasonal values of the highest maximum temperature (TXx) and seasonal values of the highest daily precipitation totals (Rx1day).
5. The second climate extremes analog was an attempt to develop a health-relevant metric and this uses four variables: seasonal 90^{th} percentile values of daily maximum temperature in austral spring (SON) and summer (DJF) and seasonal 10^{th} percentile values of daily minimum temperature in austral autumn (MAM) and winter (JJA).

Climate analogs for nine major cities were examined and their locations are shown in Figure 1a. This includes the eight state and territory capitals of Australia and Alice Springs is included as it is characterized by a different climate to all other cities studied here. In total, over 17 million people live in these nine cities.

The observations were divided into four periods of equal length: MAM 1910-DJF 1937/38, MAM 1938-DJF 1965/66, MAM 1966-DJF 1993/94, and MAM 1994-DJF 2021/22. The climate analogs were computed for each of the first three periods relative to the climate of the city of interest in the 1994-2021/22 period. The results shown here are comparing the 1910-1937/38 period with the climate of the city of interest in 1994-2021/22, but selected results for other periods are shown in Supplementary Information.

2.2. Climate analog identification

There are different methods for the identification of climate analogs. The objective of climate analogs previously has been to identify locations with similar climates in a future climate scenario to a present-day climate at a specific location. This has been done by comparing means and variability in temperature and precipitation (e.g. Bergthórsson et al., 1988). Gavin et al., (2003) compared methods for analog identification leading to subsequent studies using Standardized Euclidean Distance (SED) for the purpose of analog analysis (e.g. Veloz et al., 2012; Williams et al., 2007). SED is defined as:

$$\mathrm{SED_{ij}} = \sqrt{\sum_{k=1}^{N} \frac{\left(b_{\mathrm{ki}} - a_{\mathrm{kj}}\right)^2}{{s_{\mathrm{kj}}}^2}}$$

where N is the number of variables included analysed, a is the mean of variable k at the location of interest, j, in the recent climate, b is the mean climate under a future scenario at location, i, and $\mathrm{s_{kj}}$ is the standard deviation of climate variable k at location j. The SED is straightforward to compute and interpret aiding its' popularity for climate analog studies. In a comparison study, Grenier et al., (2013) suggested that the effects of differences between analog metrics were smaller than dependence in model selection in determining the location of the best analog.

While the SED has become well used in analog studies, it has been shown to suffer from artefacts of covariance in the variables that are used as inputs, and comparison between SED statistics based on different numbers of input variables (N in the equation for SED) is challenging (Mahony et al., 2017). Mahony et al., (2017) developed an alternative method based on standardizing the data and extracting principal components (PCs) before computing similarity in this transformed data space. This approach has been used in some subsequent analog analyses (Fitzpatrick & Dunn, 2019; Lotterhos et al., 2021).

Covariance between input variables is an issue in the Australian region as seasonal-average temperature and precipitation variability is associated with climate modes, such as the El Niño-Southern Oscillation, which may persist for multiple seasons. Also, seasonal and annual temperature and precipitation are inversely correlated in some areas of Australia (e.g. Nicholls, 2004). Thus, the SED approach is sub-optimal for examining Australian climate analogs. In this study, an adaptation of the method developed by Mahony et al., (2017) was used instead. For a given location and set of variables the following steps were taken:

1. The data for each variable at the city of interest for 1994-2021/22 were standardized based on the mean and standard deviation over the 28 values for each season in the period.

2. Mean values of all variables for 1910-1937/38 and 1938-1965/66 and 1966-1993/94 at every location were computed and then standardized using the same mean and standard deviation computed in step 1. These values are

compiled into arrays for each time period, [B$_1$'], [B$_2$'], and [B$_3$'] containing all variables.

3. An array of the standardized variables in the 1994-2021/22 period at the city of interest was compiled, [C'], and principal component analysis was performed on this array. Eight principal components (PCs) were extracted for arrays where eight variables were included and four PCs were extracted where analogs were being computed based on only four variables.

4. The arrays compiled in step 2 were projected onto all PCs so that Mahalanobis distance, D (Mahalanobis, 1936), may be computed in the transformed data space as:

$$D_{\mathrm{ij}} = \sqrt{\sum_{n=1}^{N} \frac{\left(\overline{z}_{\mathrm{in}} - y_{\mathrm{jn}}\right)^2}{{s_{\mathrm{in}}}^2}}$$

where N is the number of PCs (either 8 or 4 in this study), $\overline{z}_{\mathrm{in}}$ is the mean of each PC projected on to [C'], y_{jn} is each PC projected on to [B$_1$'], [B$_2$'], or [B$_3$'], and s_{in} is the standard deviation of each PC projected on to [C']. D may be calculated at all locations in the domain and its computation bears similarity to the SED as was used in earlier studies (e.g. Veloz et al., 2012; Williams et al., 2007), but is based on PCs of the set of variables at the city of interest rather than the raw variable data.

1. Sigma dissimilarity was computed by converting Mahalanobis distance using the Chi-distribution where the mean, , is:

$$\mu = \frac{\sqrt{2}\Gamma\left(\frac{k+1}{2}\right)}{\Gamma\left(\frac{k}{2}\right)}$$

and the standard deviation, , is

$$\sigma = \sqrt{k - \mu^2}$$

where k is the number of degrees of freedom and in this analysis, k=N as all principal components were used regardless of variance explained. For the analysis of analogs for climate means using seasonal average temperature and precipitation, and climate extreme indices, k=8, so =2.74 and =0.70. For the analysis of temperature means only, precipitation means only, and the health-related temperature extremes, k=4, so =1.88 and =0.68. The conversion of Mahalanobis distance to sigma dissimilarity allows comparability of results between analog analyses where k is different.

For fuller discussion of this methodology I refer the reader to Mahony et al., (2017). However, there are a few key differences between this study and Mahony et al., (2017) that must be highlighted. The most obvious difference is that here analogs with the recent climate were identified for past climates rather than future climates. Here, gridded observational data were used to represent the recent climate and the standard deviation in step 1 is computed from the location gridcell, whereas in Mahony et al., (2017) a collection of local station data were used. The construction of AGCD, based on interpolation of station data (Evans et al., 2020; Jones et al., 2009), means that the gridcell standard deviation is essentially derived from multiple stations, although their relative influence depends on the density of station data and the variable in question. Part of the motivation for computing analogs for major cities was that these are locations where station density is high and the climate variability in the gridded dataset should be more accurate. Also, as discussed in step 5, k=N in this analysis, whereas in Mahony et al., (2017) the higher-order principal components were not used in the Mahalanobis distance calculation. The analysis here was based on fewer principal components, so even the higher-eigenvalue PCs explain more variance than the 0.01 threshold employed for truncation of PCs by Mahony et al., (2017). This is mainly due to the analysis of four seasonal-mean temperatures rather than a combination of four seasonal-mean maximum and four seasonal-mean minimum temperatures which leads to analogs based on 8 rather than 12 variables when seasonal-total precipitation is also included.

3. Results

3.1. Climate means analysis

Sigma dissimilarity values show the level of agreement between the recent climate (1994-2021/22) of a given location and the climate at all locations further in the past (1910-1937/38). For the nine major cities analyzed here, Darwin and Perth show the biggest difference between recent and past climates at their locations at 2 and 1.6 respectively (Figure 2). As Mahony et al., (2017) point out, 2 dissimilarity equates to approximately the 95^{th} percentile of climate variability so could be considered a moderately novel climate. No sites show anything close to what Mahony et al., (2017) suggest is extremely novel, 4 dissimilarity. While other cities do not show strong dissimilarity between their recent and past climates, the best analogs to recent city climates tend to be further north for the cities in southern Australia. For example, the best early 20^{th} century analog to Sydney's recent climate is near Newcastle and the best analog to Brisbane's recent climate is near Bundaberg. Adelaide's best analog is thousands of kilometers away in southwest Western Australia. In general, the best historical analogs to present day city climates may be found in warmer locations. When the analysis was repeated comparing the recent period with later historical periods the sigma dissimilarity for Darwin and Perth decreases and the best analogs tend to move nearer to the city locations (Figures S1, S2). There is little evidence of interannual or decadal variability affecting the sigma dissimilarity patterns, despite the strong climate variability on these timescales that Australia experiences.

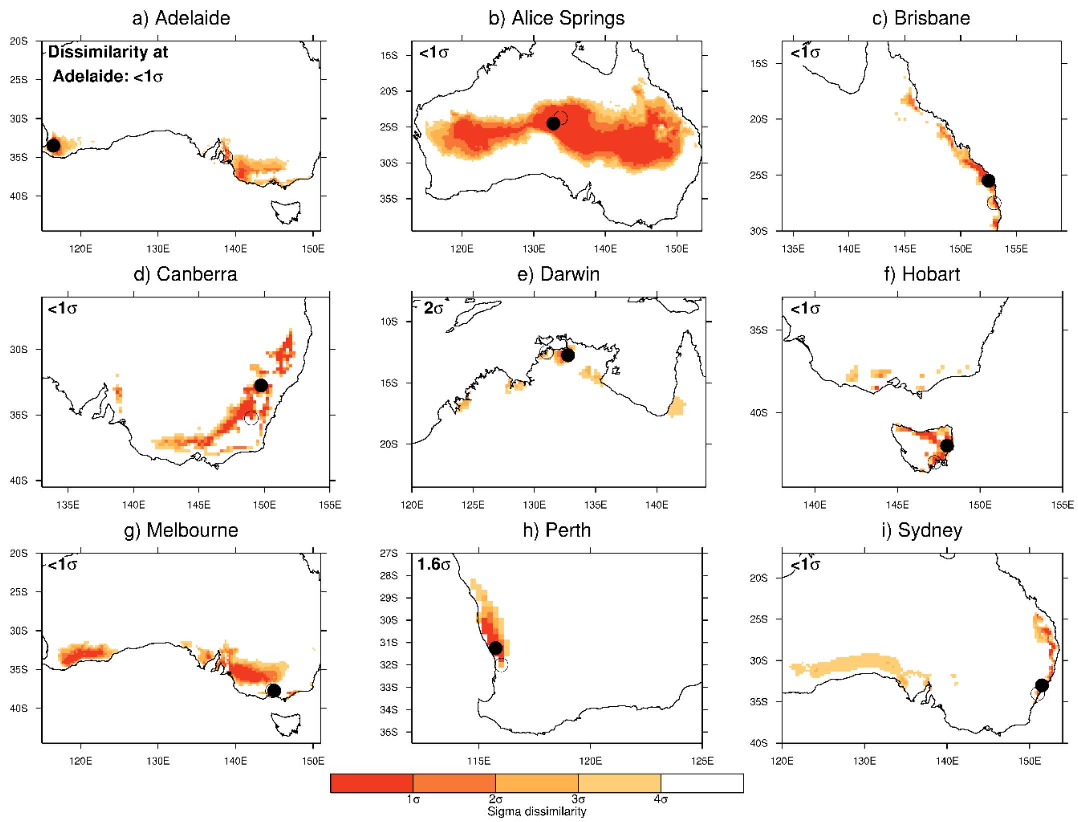

Figure 2. (a-i) Sigma dissimilarity between the city's climate in 1994-2021/22 and the climate of other locations in 1910-1937/38. The smaller the sigma dissimilarity, the more similar the climate is. The value of sigma dissimilarity between the city's climate in 1994-2021/22 and 1910-1937/38 is given in the top-left of each map. The black symbol shows the nearest analog. The unfilled circle shows the city's location.

To investigate the factors behind the identified local climate changes, the analogs were also computed for seasonal temperatures only and seasonal precipitation only. Figure 3 shows the locations of the best historical analogs from 1910-1937/38 to present-day city climates based on seasonal temperature and precipitation in combination (in black) and separately (in red and blue respectively). There are some significant differences between the temperature and precipitation analogs. For example, Melbourne's recent temperatures are most similar to those in past southeast South Australia, whereas the best rainfall analog shows no movement from Melbourne at all. For Brisbane, the best temperature and rainfall analogs are to the south, but the best climate analog is to the north. This highlights that particularly in regions of strongly variable climates, such as the eastern seaboard of Australia (Figure 1a,b), close proximity can result in very different local climates resulting in seemingly disparate movements between the best temperature, precipitation, and climate analogs.

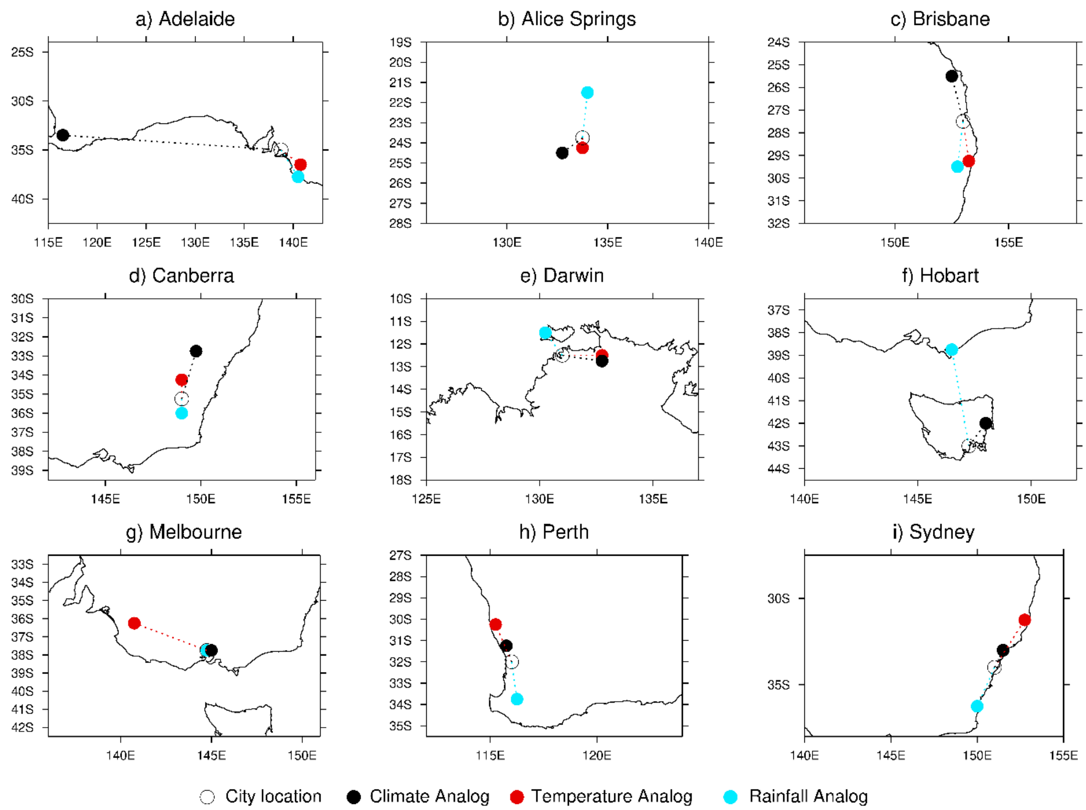

Figure 3. (a-i) Locations of the most analogous climate in 1910-1937/38 relative to each city's climate of 1994-2021/22. The black symbol shows the nearest climate analog while the red and blue symbols show the nearest analogs for temperature only and precipitation only, respectively. The unfilled circle shows the city's location.

3.2. Climate extremes analysis

Analysis on extreme climate indices (seasonal TXx and Rx1day) was also performed but showed little dissimilarity between the recent climate and historical climate of 1910-1937/38 at the city locations (Figure S3). This is due to the much higher interannual climate variability in these indices compared with the climate means. This effect is also illustrated by the broad swaths of Australia with low sigma dissimilarity values for past relative to recent city climate. The best analogs still show movement towards warmer climates. For example, the best analog for Hobart's recent climate extremes in the early 20th century is found near Sydney.

Climate analogs may take different input variables to be useful to specific stakeholders. An attempt to showcase this for temperature extremes specifically is provided here. Hot and cold extremes cause health problems and increased mortality rates including in Australia (Cheng et al., 2019; Coates et al., 2022; Gasparrini et al., 2017), although the relative importance of heat and cold for excess fatality is debated (Longden, 2019). Acclimatization is relevant to heat extremes with people more vulnerable to heat that come after cold periods (Nairn et al., 2014). Thus, the 90th percentile of seasonal maximum temperatures in spring and summer, and the 10th percentile of seasonal minimum temperatures in autumn and winter were used as input variables for a health-relevant climate analog.

The input variables in this case have lower interannual variability than TXx and Rx1day, so the sigma dissimilarity is broadly higher (Figure 4). Darwin is still the only city to have transitioned to experiencing a truly novel climate with respect to this health-relevant analog with local dissimilarity of 3.2 between the recent period and 1910-1937/38 window. However, as with the climate means analog, the best health-relevant analogs are in warmer locations than the city of interest. For example, Sydney's health-relevant climate analog for the 1994-2021/22 period is a location near Brisbane in the 1910-1937/38 period. There is potential for stakeholders to use climate analogs information to understand the challenges their sector may face in the current climate.

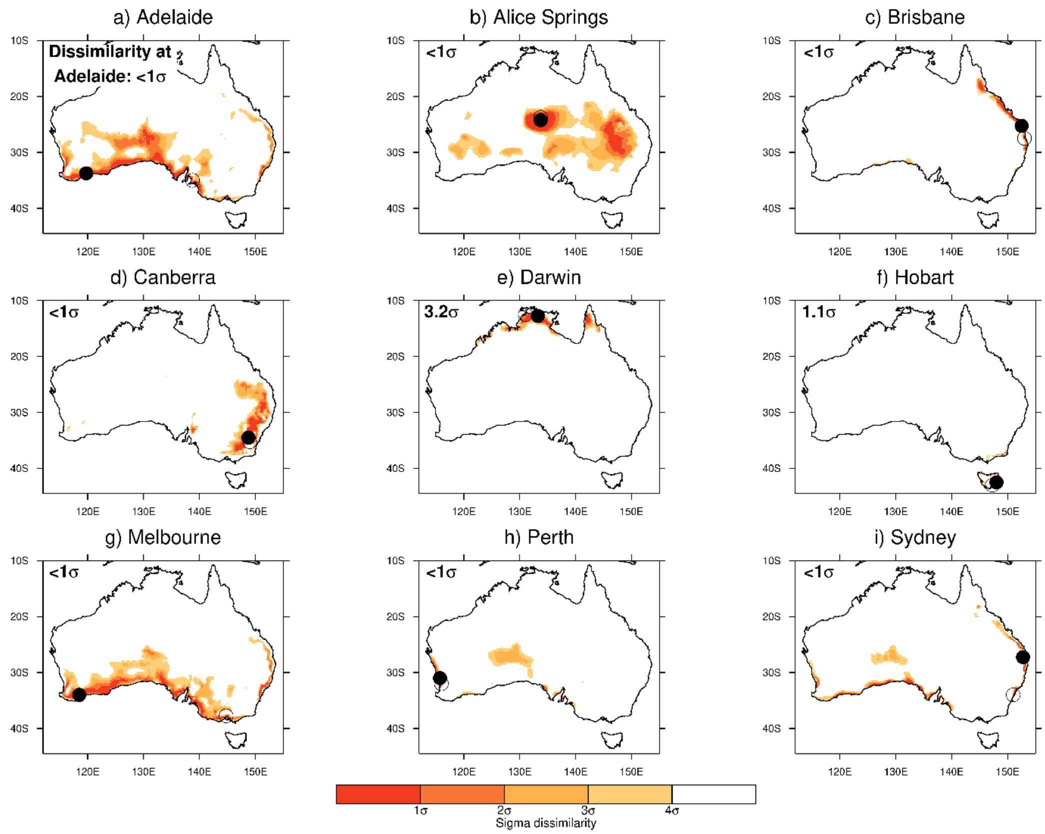

Figure 4. (a-i) Sigma dissimilarity between the city's temperature extremes in 1994-2021/22 and the temperature extremes of other locations in 1910-1937/38. The value of sigma dissimilarity between the city's temperature extremes in 1994-2021/22 and 1910-1937/38 is given in the top-left of each map. The black symbol shows the nearest analog. The unfilled circle shows the city's location.

4. Discussion and Conclusions

This analysis is the first, to the author's knowledge, to apply climate analog techniques to study past climate changes in the instrumental period rather than future climate scenarios. Through using an adapted version of the Mahony et al., (2017) methodology, climate analogs were computed and significant changes in climate were identified, particularly in Darwin and Perth while other major Australian cities experienced more subtle changes between the early 20$^{\text{th}}$ century and recent period. Darwin was the only tropical location studied here and showed the strongest climate shift in the observational record using both the mean climate analog and the health-relevant analog. In general, climate changes in the tropics are clearer than in high-latitude regions due to lower interannual variability (Diffenbaugh & Scherer, 2011; Hawkins et al., 2020; Mahlstein et al., 2011). Perth has experienced significant rainfall decline (Delworth & Zeng, 2014; Hope et al., 2006) as well as the warming that has been observed in all major Australian cities and this has contributed to the high dissimilarity between current and past Perth climate. As the climate continues to change, analogs could be updated. Seamless analysis of past and future analogs could also be conducted by blending observations, high-resolution reanalyses and projections.

Climate analogs for extremes indices were explored in this study. In general, the high interannual variability in climate extremes reduces sigma dissimilarity values between present and past climates but shifts in best analogs to warmer locations are still identified. Australia has experienced significant increases in the frequency and intensity of heat extremes over the past century (Alexander & Arblaster, 2017; Lewis & King, 2015; Perkins & Alexander, 2013), while changes in rainfall extremes have been less clear and are more complex (Alexander & Arblaster, 2017; Dey et al., 2019, 2020).

This study uses only observational data to explore historical climate analogs. Thus, the cause of movements in the best analog and the sigma dissimilarity statistics cannot be directly attributed to anthropogenic climate change here. However, the underlying warming of Australia (Eyring et al., 2021) and increased frequency and intensity of hot extremes (Seneviratne et al., 2021) have been attributed to anthropogenic forcings previously. This study adds a new way of framing historical climate changes in Australia.

This study focused on only major Australian cities where there is a reasonable density of weather stations (Jones et al., 2009). Extending climate analog analysis to rural locations could be useful, particularly if analogs are designed with stakeholders such as local agriculture or water management, but would be susceptible to issues with data quality. The application of climate analogs to specific stakeholders requires careful thought and co-design between scientists and sectoral experts. The example of a health-relevant analog in this study is illustrative and would require refinement for further use.

This work has shown that climate analogs may be used to identify past climate changes as well as for communication of projections. Further work to make historical analogs relevant to stakeholder interests could be beneficial.

Acknowledgements

The author received support from the Australian Government National Environmental Science Program. The work was undertaken with the assistance of resources from the National Computational Infrastructure (NCI), which is supported by the Australian Government.

Open Research

The Australian Gridded Climate Dataset is available on NCI: http://climate-cms.wikis.unsw.edu.au/AGCD (Australian Bureau of Meteorology, 2020a).

The code and netCDF files generated in this analysis are provided here: https://doi.org/10.5281/zenodo.7179190.

References

Alexander, L. V., & Arblaster, J. M. (2017). Historical and projected trends in temperature and precipitation extremes in Australia in observations and CMIP5. *Weather and Climate Extremes*, *15*, 34–56. https://doi.org/10.1016/J.WACE.2017.02.001Australian Bureau of Meteorology. (2020a). Australian Gridded Climate Data (AGCD) ; v2.0.0 Snapshot (1900-01-01 to 2020-05-31). Retrieved October 10, 2022, from http://dx.doi.org/10.25914/6009600786063Australian Bureau of Meteorology. (2020b). *State of The Climate 2020*. Melbourne. Retrieved from http://www.bom.gov.au/state-of-the-climate/documents/State-of-the-Climate-2020.pdfBergthórsson, P., Björnsson, H., Dýrmundsson, Ó., Gudmundsson, B., Helgadóttir, A., & Jónmundsson, J. V. (1988). The effects of climatic variations on agriculture in Iceland. In M. Parry, T. Carter, & N. Konijn (Eds.), *The impact of climatic variations on agriculture. Volume 1: Assessments in cool temperate and cold regions.* (pp. 381–509). Kluwer Academic Publishers.Cheng, J., Xu, Z., Bambrick, H., Su, H., Tong, S., & Hu, W. (2019). Impacts of heat, cold, and temperature variability on mortality in Australia, 2000–2009. *Science of The Total Environment*, *651*, 2558–2565. https://doi.org/10.1016/J.SCITOTENV.2018.10.186Coates, L., van Leeuwen, J., Browning, S., Gissing, A., Bratchell, J., & Avci, A. (2022). Heatwave fatalities in Australia, 2001–2018: An analysis of coronial records. *International Journal of Disaster Risk Reduction*, *67*, 102671. https://doi.org/10.1016/J.IJDRR.2021.102671Davis, S. J., Liu, Z., Deng, Z., Zhu, B., Ke, P., Sun, T., et al. (2022). Emissions rebound from the COVID-19 pandemic. *Nature Climate Change 2022*, *12*, 412–414. https://doi.org/10.1038/s41558-022-01332-6Delworth, T. L., & Zeng, F. (2014). Regional rainfall decline in Australia attributed to anthropogenic greenhouse gases and ozone levels. *Nature Geoscience*, *7*(8), 583–587. https://doi.org/10.1038/ngeo2201Dey, R., Lewis, S. C., Arblaster, J. M., & Abram, N. J. (2019, May 1). A review of past and projected changes in Australia's rainfall. *Wiley Interdisciplinary Reviews: Climate Change*. Wiley-Blackwell. https://doi.org/10.1002/wcc.577Dey, R., Gallant, A. J. E., & Lewis, S. C. (2020). Evidence of a continent-wide shift of episodic rainfall in Australia. *Weather and Climate Extremes*, *29*, 100274. https://doi.org/10.1016/j.wace.2020.100274Diffenbaugh, N. S., & Scherer, M. (2011). Observational and model evidence of global emergence of permanent, unprecedented heat in the 20th and 21st centuries. *Climatic Change*, *107*(3), 615–624. https://doi.org/10.1007/s10584-011-0112-yEvans, A., Jones, D., Smalley, R., & Lellyett, S. (2020). *An enhanced gridded rainfall analysis scheme for Australia*. Melbourne. Retrieved from http://www.bom.gov.au/research/publications/researchreports/BRR-041.pdfEyring, V., Gillett, N., Achuta Rao, K., Barimalala, R., Barreiro Parrillo, M., Bellouin, N., et al. (2021). Human Influence on the Climate System. In V. Masson-Delmotte, P. Zhai, A. Pirani, S. Connors, C. Péan, S. Berger, et al. (Eds.), *Climate Change 2021: the Physical Science Basis. Contribution of Working Group 1 to the Sixth Assessment Report of the Intergovernmental Panel on Climate Change* (pp. 423–552). Cambridge, UK and New York, USA: Cambridge University Press. https://doi.org/10.1017/9781009157896.005Fitzpatrick, M. C., & Dunn, R. R. (2019). Contemporary climatic analogs for 540 North American urban areas in the late 21st century. *Nature Communications 2019 10:1*, *10*(1), 1–7. https://doi.org/10.1038/s41467-019-08540-3Friedlingstein, P., Jones, M. W., O'Sullivan, M., Andrew, R. M., Bakker, D. C. E., Hauck, J., et al. (2022). Global Carbon Budget 2021. *Earth System Science Data*, *14*(4), 1917–2005. https://doi.org/10.5194/ESSD-14-1917-2022Gasparrini, A., Guo, Y., Sera, F., & al., et. (2017). Projections of temperature-related excess mortality under climate change scenarios. *Lancet Planet Health*, *1*, e360–e367.Gavin, D. G., Oswald, W. W., Wahl, E. R., & Williams, J. W. (2003). A statistical approach to evaluating distance metrics and analog assignments for pollen records. *Quaternary Research*, *60*, 356–367. https://doi.org/10.1016/S0033-5894(03)00088-7Grenier, P., Parent, A. C., Huard, D., Anctil, F., & Chaumont, D. (2013). An Assessment of Six Dissimilarity Metrics for Climate Analogs. *Journal of Applied Meteorology and Climatology*, *52*(4), 733–752. https://doi.org/10.1175/JAMC-D-12-0170.1Hawkins, E., Frame, D., Harrington, L., Joshi, M. M., King, A. D., Rojas, M., & Sutton, R. (2020). Observed Emergence of the Climate Change Signal: From the Familiar to the Unknown. *Geophysical Research Letters*, *47*(6). https://doi.org/10.1029/2019GL086259Hope, P. K., Drosdowsky, W., & Nicholls, N. (2006). Shifts in the synoptic systems influencing southwest Western Australia. *Climate Dynamics*, *26*(7–8), 751–764. https://doi.org/10.1007/s00382-006-0115-yIPCC. (2021). Summary for Policymakers. In V. Masson-Delmotte, P. Zhai, A. Pirani, S. Connors, C. Péan, S. Berger, et al. (Eds.), : *Climate Change 2021: The Physical Science Basis. Contribution of Working Group I to the Sixth Assessment Report of the Intergovernmental Panel on Climate Change* (pp. 3–32). Cambridge, United Kingdom and New York, USA: Cambridge University Press. https://doi.org/10.1017/9781009157896.001Jones, D. A., Wang, W., & Fawcett, R. (2009). High-quality spatial climate data-sets for Australia. *Australian Meteorological and Oceanographic Journal*, *58*, 233–248. Retrieved from http://www.bom.gov.au/jshess/docs/2009/jones_hres.pdfKalkstein, L. S., & Greene, J. S. (1997). An evaluation of climate/mortality relationships in large U.S. cities and the possible impacts of a climate change. *Environmental Health Perspectives*, *105*(1), 84–93. https://doi.org/10.1289/EHP.9710584King, A. D., Peel, J., Ziehn, T., Bowen, K. J., McClelland, H. L. O., McMichael, C., et al. (2022). Preparing for a post-net-zero world. *Nature Climate Change 2022 12:9*, *12*(9), 775–777. https://doi.org/10.1038/s41558-022-01446-xLewis, S. C., & King, A. D. (2015). Dramatically increased rate of observed hot record breaking in recent Australian temperatures. *Geophysical Research Letters*, *42*(18), 7776–7784. https://doi.org/10.1002/2015GL065793Longden, T. (2019). Temperature-related mortality and climate change in Australia.

The Lancet Planetary Health, *3*(3), e121. https://doi.org/10.1016/S2542-5196(19)30016-6Lotterhos, K. E., Láruson, Á. J., & Jiang, L. Q. (2021). Novel and disappearing climates in the global surface ocean from 1800 to 2100. *Scientific Reports 2021 11:1*, *11*(1), 1–16. https://doi.org/10.1038/s41598-021-94872-4MacDougall, A. H., Frölicher, T. L., Jones, C. D., Rogelj, J., DamonMatthews, H., Zickfeld, K., et al. (2020). Is there warming in the pipeline? A multi-model analysis of the Zero Emissions Commitment from CO2. *Biogeosciences*, *17*(11), 2987–3016. https://doi.org/10.5194/BG-17-2987-2020Mahalanobis, P. C. (1936). On the Generalized Distance in Statistics. *Proceedings of the National Institute of Sciences of India*, *2*, 49–55. Retrieved from http://library.isical.ac.in:8080/jspui/bitstream/10263/6765/1/Vol02_1936_1_Art05-pcm.pdfMahlstein, I., Knutti, R., Solomon, S., & Portmann, R. W. (2011). Early onset of significant local warming in low latitude countries. *Environmental Research Letters*, *6*(3), 034009. https://doi.org/10.1088/1748-9326/6/3/034009Mahlstein, I., Hegerl, G., & Solomon, S. (2012). Emerging local warming signals in observational data. *Geophysical Research Letters*, *39*(21), n/a-n/a. https://doi.org/10.1029/2012GL053952Mahony, C. R., Cannon, A. J., Wang, T., & Aitken, S. N. (2017). A closer look at novel climates: new methods and insights at continental to landscape scales. *Global Change Biology*, *23*(9), 3934–3955. https://doi.org/10.1111/GCB.13645Nairn, J. R., Fawcett, R. J. B., Ebi, K. L., & Hess, J. (2014). The Excess Heat Factor: A Metric for Heatwave Intensity and Its Use in Classifying Heatwave Severity. *International Journal of Environmental Research and Public Health 2015, Vol. 12, Pages 227-253*, *12*(1), 227–253. https://doi.org/10.3390/IJERPH120100227Nicholls, N. (2004). The Changing Nature of Australian Droughts. *Climatic Change*, *63*(3), 323–336. https://doi.org/10.1023/B:CLIM.0000018515.46344.6dPeel, M. C., Finlayson, B. L., & Mcmahon, T. A. (2007). Hydrology and Earth System Sciences Updated world map of the Köppen-Geiger climate classification. *Hydrol. Earth Syst. Sci*, *11*, 1633–1644. Retrieved from www.hydrol-earth-syst-sci.net/11/1633/2007/Perkins, S. E., & Alexander, L. V. (2013). On the Measurement of Heat Waves. *Journal of Climate*, *26*(13), 4500–4517. https://doi.org/10.1175/JCLI-D-12-00383.1Seneviratne, S. I., Zhang, X., Adnan, M., Badi, W., Dereczynski, C., Di Luca, A., et al. (2021). Weather and Climate Extreme Events in a Changing Climate . In V. Masson-Delmotte, P. Zhai, A. Pirani, S. L. Connors, C. Pean, S. Berger, et al. (Eds.), *Climate Change 2021: The Physical Science Basis. Contribution of Working Group I to the Sixth Assessment Report of the Intergovernmental Panel on Climate Change* (pp. 1513–1766). Cambridge, UK and New York, USA: Cambridge University Press. https://doi.org/10.1017/9781009157896.013Veloz, S., Williams, J. W., Lorenz, D., Notaro, M., Vavrus, S., & Vimont, D. J. (2012). Identifying climatic analogs for Wisconsin under 21st-century climate-change scenarios. *Climatic Change*, *112*(3–4), 1037–1058. https://doi.org/10.1007/S10584-011-0261-Z/TABLES/3Webb, L. B., Watterson, I., Bhend, J., Whetton, P. H., & Barlow, E. W. R. (2013). Global climate analogues for winegrowing regions in future periods: projections of temperature and precipitation. *Australian Journal of Grape and Wine*

Research, *19*(3), 331–341. https://doi.org/10.1111/AJGW.12045Williams, J. W., Jackson, S. T., & Kutzbach, J. E. (2007). Projected distributions of novel and disappearing climates by 2100 AD. *Proceedings of the National Academy of Sciences of the United States of America*, *104*(14), 5738–5742. https://doi.org/10.1073/PNAS.0606292104/SUPPL_FILE/06292FIG7.PDF